Journal of Climate Change, Vol. 6, No. 1 (2020), pp. 37-46.
DOI 10.3233/JCC200005

Reconstruction of the Paleoenvironmental Condition Using Geochemical Proxies in the Lower Baitarani Basin, Coastal Odisha, India

Uzma Parveen[1], S. Sreekesh[1]* and Sandeep Sarpal[2]

[1]Centre for the Study of Regional Development, Jawaharlal Nehru University, New Delhi
[2]Advanced Instrumentation Research Facility, Jawaharlal Nehru University, New Delhi
✉ sreekesh@mail.jnu.ac.in

Received October 2, 2019; revised and accepted January 27, 2020

Abstract: The subsurface sediment archives provide clues to the past climate of the Earth. To reconstruct the paleoclimate of Lower Baitarani Basin, a 1000 cm deep sediment core (JP) was collected from the flood plain located in Jhumpuri village of Jajpur, Odisha. A total number of eleven distinct layers were identified based on variations in the sediment colour and textural at varying depths. From each layer, a representative sample was collected and carried to the laboratory for further assessment. Each of these sub-samples was examined for particle size analysis, availability of total organic carbon (TOC), and elemental concentration. The physical and geochemical proxies as paleoproductivity, terrestrial flux, weathering, level of salinity, colour, and texture variations were utilised to examine the paleoclimate of the area. The colour variations of the subsurface sequences suggest that the deposition has occurred under both freshwater and stagnated/marshy conditions. The texture variations—clay, silty clay, and loamy fine sand—also indicate deviations in sediment supply and rate of sediment aggradation during climatic shift between warm-humid and cold-arid episodes.

With the help of geochemical proxies to illustrate the terrestrial flux: Fe_2O_3, Al_2O_3, TiO_2, MgO, CaO, Cu, Co, Ba, and Zn; paleoproductivity: TOC,CaO/Al_2O_3, Zn/Al_2O_3, Sr/Al_2O_3, Cu/Al_2O_3, and Ba/Al_2O_3; weathering: Fe_2O_3/Al_2O_3, TiO_2/Al_2O_3, and MgO/Al_2O_3; and the salinity index, a relatively cold-dry climate is inferred during the sedimentation of basal layers. Subsequently, a shift to the relatively warm-humid phase is suggested which again was followed by a cold-dry, and warm-humid phases. In the recent deposits, the proxies have not shown any considerable variation indicating prolongation of the existing warm-humid phase. However, some indications of a climatic shift to colder climate is also marked in the surface layer (JPL1).

Keywords: Paleoclimate; Geochemical proxies; Grain size; Sedimentation; Flood plain.

Introduction

Climate of the Earth has changed throughout the geological time either in the form of drastic changes over millions of years or as minor fluctuations (Juyal et al., 2003; Jayalakshmi et al., 2004; Kumaran et al., 2005; Anderson et al., 2007; Nair et al., 2010). Due to absence of long-term direct climatic records, the paleoclimatic changes are inferred using proxy sources (Vaz and Banerjee, 1997; Roberts, 1998; Alappat et al., 2011; Jayangondaperumal et al., 2012; Srivastava and Farooqui, 2013; Tripathi et al., 2014; Limaye et al., 2014; Malik et al., 2015; Rao et al., 2015; Govil et al., 2016; Makwana et al., 2019). A cautious examination of the landform stratigraphy also yields clues to the past climate (Babu, 1975; Banerjee et al., 1993; Chauhan

*Corresponding Author

et al., 1993; Agnihotri et al., 2003; Banerjee, 2000; Kumaran et al., 2005; Coltorti et al., 2010; Farooqui and Naidu, 2010; Rao et al., 2012; Selvakumar et al., 2012; Singh et al., 2014; Alappat et al., 2015; Basaviah et al., 2015; Das et al., 2017; Narayana et al., 2017).

The analysis of stratigraphic archives is a relative method of paleoclimate reconstruction. The textural variability of sediments in a stratigraphic sequence reflects the mode of sediment transportation and environment of deposition over time and space yielding crucial information about the past climate (Naguib and Bedaiwy, 2012). Even though this approach does not provide exact age, it offers crucial information about the depositional history, rate of sedimentation, changes interrestrial flux, and degree of weathering (Banerji et al., 2017; Narayana, 2017). The variation in Fe_2O_3, Al_2O_3, TiO_2, Co, Cu, Zn, CaO, Ba, and MgO concentration represents changes in the terrestrial flux indirectly indicating deviations in humidity (Banerji et al., 2017).

The geochemical proxies i.e. total organic carbon (TOC), CaO/Al_2O_3, and Cu/Al_2O_3 are used to analyze the varying paleoproductivity in the region (Scneider et al., 1997; Mohtadi and Hebbeln, 2004; Haiyan et al., 2010; Govil et al., 2016) which is considered a crucial indicator of dry/wet as well as warm/cold climatic episodes (Govil et al., 2016). The oscillating paleoproductivity is associated with the distinct climatic set-up making it a common tool for paleoclimatic reconstruction (Sageman and Lyons, 2003). The paleo-weathering and salinity, similarly, reflect changes in the depositional environment (Banerji et al., 2017). In this backdrop, the present study attempts to analyse the paleoclimate using geochemical proxies as well as their relevance in revealing the past climate.

Study Area

The area of study is located in the flood plain of Baitarani River between 2049′52.5″° latitude and 8626′40.5″° longitude in Jhumpuri village of Odisha (Figure 1). The general elevation of this site is 10 m above the mean sea level. It is located around 55 km away from the Bay of Bengal. The study area falls under

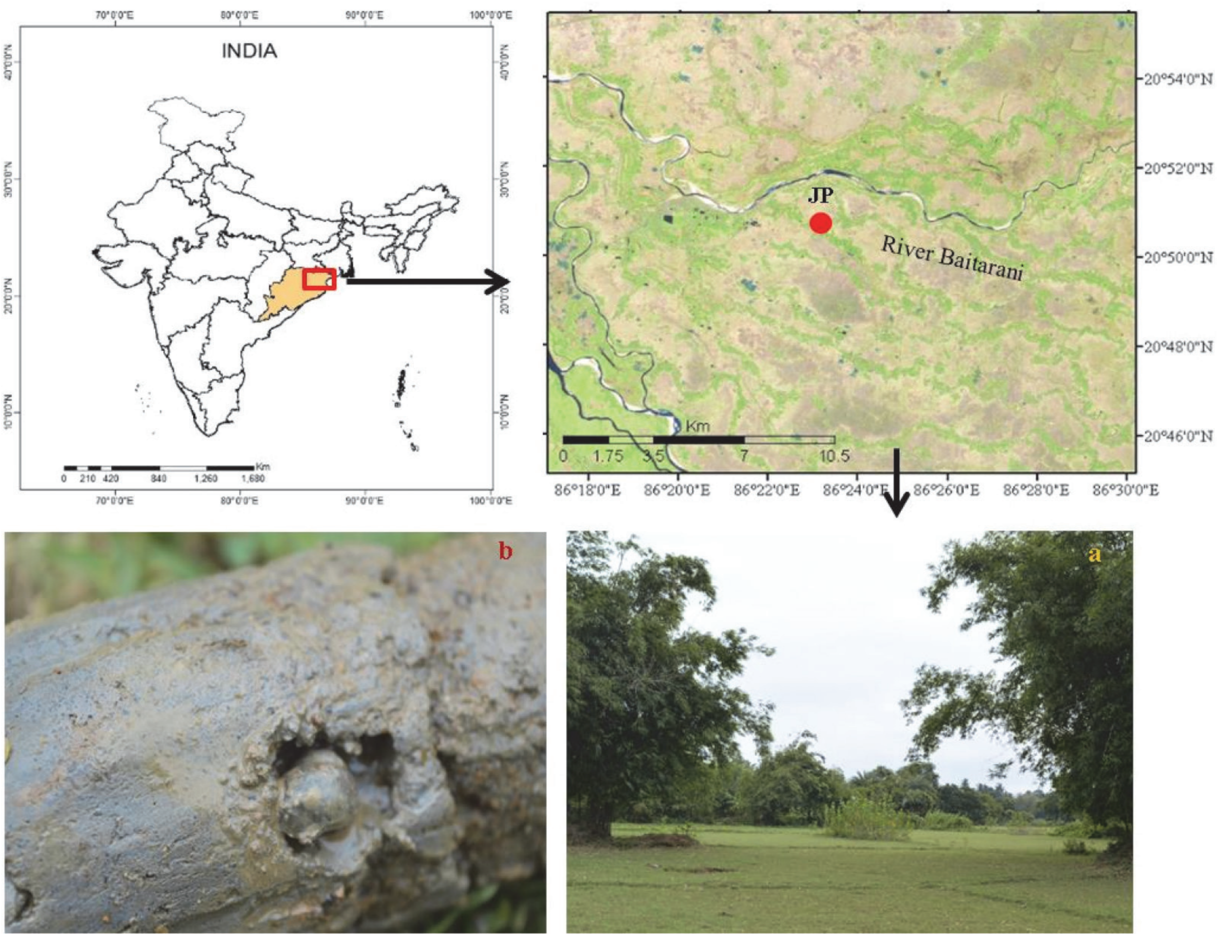

Figure 1: Area of study: (a) sample collection site and (b) shell in the subsurface layer of JPS6.

a zone of subtropical monsoon climate with distinct summer, monsoon and winter seasons. The mean annual rainfall is 1568.4 mm, which is mainly received from the south-west monsoon. From geological perspective, this area is a part of the eastern coastal plain formed by younger, unconsolidated deposits of the Tertiary and Quaternary periods (Banerjee, 2000). The coastal plain, where the sample collection site is located, is comprised of the fluvio-marine deposits (Banerjee, 1993; Islam and Tooley, 1999; Hameed et al., 2006; Khandelwal et al., 2008).

Methodology

Collection of Sub-surface Samples and Sampling

A sub-surface sediment core was acquired from the floodplain of river Baitarani at Jajpur district, Odisha. A total number of eleven distinct layers were identified based on varying colour and sediment texture. All the eleven sub-samples collected from representative layers were inspected for grain size analysis, TOC, and the assessment of elemental concentration.

Colour and Grain Size Analysis

The colour identification of each sub-sample is based on Munsell colour chart (Munsell, 1930). The grain size analysis was performed using a 151 H-hydrometer (Naguib and Bedaiwy, 2012). For this, each of the samples was oven-dried at a temperature of 105°C for about 24 hours. Around 50 g of the dried sample was passed through a sieve of 2 mm to extract the rock and wood particles from the sample. Sodium hexametaphosphate $(NaPO_3)_6$ solution was obtained by mixing 50 g of $(NaPO_3)_6$ with distilled water. Further, 100 ml of this solution and 250 ml of distilled water was mixed with soil samples and kept overnight. Subsequently, the samples were mixed using a mixing machine for 5 minutes and poured into a 1000 ml measuring cylinder. After 30 seconds, the first temperature and hydrometer reading was taken. Thereafter, temperature and hydrometer readings were noted at the interval of 60 seconds, 1.5 hours, 4 hours, 8 hours, and 24 hours. A blank sample was also prepared for calibration. The availability of sand, clay and silt (in percentage) was calculated using the following formula:

$$\%\ \text{sand} = \frac{100 - (\text{Reading 30 second} \times 2 - \text{Blank reading})}{\text{Oven dried weight of soil}} \times 100 \quad (1)$$

$$\%\ \text{clay} = \frac{(\text{Reading 4 hour} \times 2 - \text{Blank reading})}{\text{Oven dried weight of soil}} \times 100 \quad (2)$$

$$\%\ \text{silt} = 100 - (\text{sand}\ \% + \text{clay}\ \%) \quad (3)$$

TOC and Concentration of Elements

The TOC concentration is analyzed using Walkley-Black method suggested by Walkley and Black, (1934) at the soil laboratory of the Institute of Agriculture, Banaras Hindu University, Varanasi, India. The elemental concentration in the sediment samples is assessed through Energy Dispersive X-Ray Fluorescence (EDXRF), at Advanced Instrumentation Research Facility (AIRF), JNU, New Delhi.

Proxies for Terrestrial Flux, Paleoproductivity, Past Weathering and Salinity

In this study, the analysis of paleoclimate is based on the inferences drawn from the geochemical proxies i.e. variations in terrestrial/detrital flux, paleoproductivity, weathering, and level of salinity. Fluctuation in these indicators also demonstrates the variation in tidal/marine influences in the region. The variability of Fe_2O_3, Al_2O_3, TiO_2, MgO, CaO, Cu, Co, Ba, and Zn in the subsurface layers is utilized as tracers of terrestrial flux (Banerji et al., 2017). Fe_2O_3, Al_2O_3, TiO_2, Cu, Co, and Zn are generally derived from detrital sources whereas the elements such as Ba, CaO, and MgO are obtained from biogenic sources (Gredilla et al., 2015; Li et al., 2019). The availability of elements received from the terrestrial sources tend to increase under a humid climate due to enhanced fluvial processes in the catchment while their availability declines under a relatively arid climate marked by lower sediment supply. In contrast, the concentration of Ba, MgO, and CaO increases under the increasing marine/tidal activities in coastal regions and declines under reduced marine action.

The down core variation in TOC and CaO/Al_2O_3, Zn/Al_2O_3, Sr/Al_2O_3, Cu/Al_2O_3, and Ba/Al_2O_3 ratios are used to evaluate the changes in past primary productivity or paleoproductivity (Goldberg and Arrhenius, 1958; Agnihotri et al., 2003; Tribovillard et al., 2006).The biological productivity is usually high during the warm-humid phase whereas it reduces under a cold-dry climate (Hodgson et al., 2003; Govil et al., 2016).

The ratios of Fe_2O_3/Al_2O_3, TiO_2/Al_2O_3, and MgO/Al_2O_3 are utilised as proxies to examine the deviations in paleo-weathering (Banerje et al., 2017; Liu et al., 2019). The past changes in salinity is evaluated using the salinity index: MgO/CaO+MgO (Banerji et al., 2017). Thus, the selected geochemical proxies are related directly or indirectly with the changes in temperature and humidity conditions of the region.

Results and Discussion

Sediment Stratigraphy

The lithological log represents eleven major sediment sequences with distinct colour and/or texture (Figure 2). The JPS1 is dark reddish-brown, JPS2 is dull reddish-brown, JPS3 is yellow, JPS4 is reddish-gray, JPS5 is reddish-black, JPS6 is grayish-red, JPS7 is brownish-black, JPS8 is grayish yellow, JPS9 is pale reddish-orange, JPS10 is dull-orange, and JPS11 is grayish-white (Table 1).The red colour of the sediments indicates abundance of iron under a dry or well-oxygenated environment (Koukina et al., 2017; Sayem et al., 2018). The orange-brown colour of the sediments indicates a higher supply of iron (Fe) and manganese (Mn) oxides (Koukina et al., 2017). The dark brown and black sequences are the result of inadequately oxygenated organic matter or a deep water/swampy environment. The gray colour illustrates the deficiency of oxygen under a persistent waterlogged or swampy conditions (Kobayashi et al., 2016). Thus, the colour scheme of the sub-surface sediment sequences at JP site has indicated deposition under both well-oxygenated and reducing conditions.

The texture of the sub-surface sediments has varied considerably (Table 1). The JPS1, JPS3, JPS5, JPS6 and JPS8 are clay, JPS2 is silty clay, JPS4 is loamy fine sand, and remaining layers (JPS7, JPS9, JPS10 and JPS11) are fine sand. The textural distinctiveness indicates that the sediment accumulation has occurred under a relatively warm-humid and cold-dry climatic conditions. The clayey layers have been linked with the relatively warm-humid environment, as the length of the river tends to extend further in the coastal areas due to an increase in stream flow capacity while under a drier climate river course is shortened and marine influence increases (Krishna, 2017).

Distribution of TOC and Selected Elements

The distribution of TOC has deviated from 0.06 to 0.75% (Table 2). Among major elements, the concentration of MgO has varied from 2.17 to 2.54 %, Al_2O_3 from 10.7 to 13.6%, CaO from 2.48 to 3.56%, TiO_2 from 0.24 to 0.96%, and Fe_2O_3 from 5.82 to 17.4%. Among trace elements, Co has fluctuated from 13 to 25 ppm, Cu from 26 to 67 ppm, Zn from 3.0 to 103 ppm, and Ba from 324 to 520 ppm.

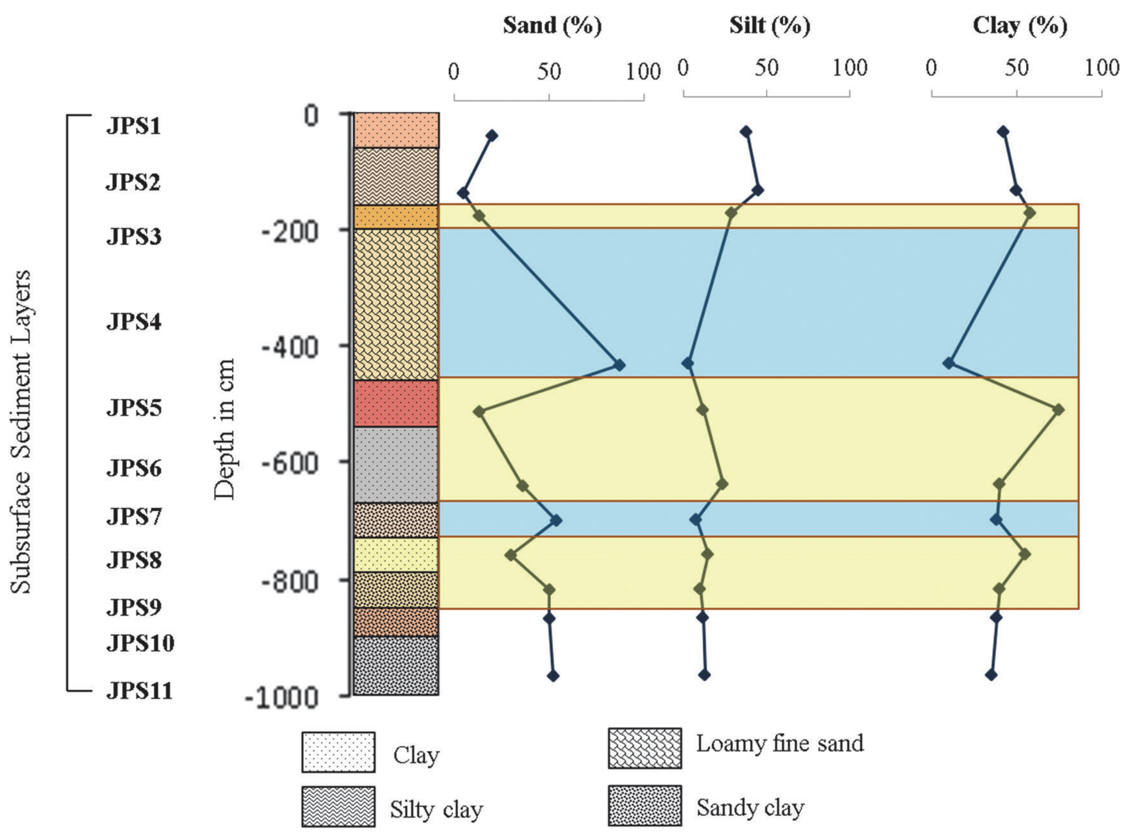

Figure 2: Subsurface sediment layers, lithological log and concentration of sand, silt and clay in different layers. The yellow rectangles are showing warm-humid while blue rectangles are showing cold-dry climatic episodes.

Table 1: Colour and textural variability of subsurface sediment layers

Layers	*JPS1*	*JPS2*	*JPS3*	*JPS4*	*JPS5*	*JPS6*	*JPS7*	*JPS8*	*JPS9*	*JPS10*	*JPS11*
Depth (cm)	0-60	60-160	160-200	200-460	460-540	540-670	670-730	730-790	790-850	850-900	900-1000
Colour	Dark reddish brown	Dull reddish brown	Yellow	Reddish gray	Reddish black	Grayish red	Brownish black	Grayish yellow	Pale reddish orange	Dull orange	Grayish white
Texture	Clay	Silty clay	Clay	Loamy fine sand	Clay	Clay	Sandy clay	Clay	Sandy clay	Sandy clay	Sandy clay

Table 2: Concentration of TOC, major (%) and trace elements (ppm) in the subsurface sediments of JP

Elements/Layers	*JPS1*	*JPS2*	*JPS3*	*JPS4*	*JPS5*	*JPS6*	*JPS7*	*JPS8*	*JPS9*	*JPS10*	*JPS11*
TOC (%)	0.33	0.11	0.06	0.26	0.63	0.33	0.75	0.56	0.54	0.08	0.09
Al_2O_3	11.7	11.3	12.1	11.2	13.7	13.6	11.8	10.7	12.4	11.7	12.3
CaO	2.95	2.96	2.97	2.48	3.06	2.95	3.10	3.56	3.05	2.97	3.0
TiO_2	0.88	0.90	0.96	0.24	0.92	0.74	0.53	0.79	0.75	0.52	0.67
MgO	2.42	2.48	2.37	2.51	2.17	2.19	2.42	2.54	2.33	2.44	2.37
Co (ppm)	23	21	23	17	25	21	17	21	14	13	16
Cu	53	49	56	37	67	51	30	41	41	34	26
Zn	66	73	79	23	103	63	11	60	7.0	3.0	13
Ba	466	496	497	385	393	384	324	520	479	385	386

Reconstruction of Paleoclimate

Variations in Terrestrial Flux

The terrestrial flux represented by Fe_2O_3, Al_2O_3, TiO_2, Cu, Co and Zn is low during the deposition of JPS11 and JPS10 suggesting a relatively lower humidity and hence a comparatively cold-dry climatic phase (Figure 3). During the accumulation of JPS9, the terrestrial flux began to increase, which can be attributed to the increase in rainfall and a transition in climate towards warm-humid phase. At this time, the content of Ba and MgO was relatively low suggesting a declining influence of tidal activity. A relatively higher terrestrial flux in JPL8 suggests the existence of a warm-humid climate. A decline in the terrestrial flux during the aggradation of JPS7 demonstrates a lower humidity under a relatively cold-dry climate. The increasing concentration of Ba and MgO in this layer suggests a rise in tidal influence. The terrestrial flux increased markedly during the deposition of JPS5 signifying a higher humidity and decline in the tidal influence under warm-humid climate. In succeeding layer, JPL4, are markable reduction in the terrestrial flux can be associated with a declining humidity under the cold-dry climate. During the sedimentation of JPS3, an enhanced terrestrial flux can be attributed to the warm-humid climate. In JPS2, and JPS1 layers, the terrestrial flux has not shown any considerable fluctuation, which might be associated with a transitioning climate.

Variations in Paleoproductivity

The geochemical proxies, TOC, Ca/Al_2O_3, Cu/Al_2O_3, Ba/Al_2O_3, and Zn/Al_2O_3 indicate a relatively low paleoproductivity in JPS11 and JPS10, which can be associated with a cold-dry climate (Figure 4). The proxies illustrate a rise in paleoproductivity during the aggradation of JPS9, indicating a transitioning phase. A higher paleoproductivity during the deposition of JPS8 illustrates the existence of a warm and humid climate. Afterward, the paleoproductivity has declined as represented by TOC, CaO/Al_2O_3, Cu/Al_2O_3, Zn/Al_2O_3, Sr/Al_2O_3, and Ba/Al_2O_3 in JPS6 revealing another episode of the cold-dry climate. In JPS5, an increase in paleoproductivity indicates a warm-humid climate. Another period of declining paleoproductivity is marked in JPS4, which again can be related with a relatively cold and dry episode. In JPS3, the indicators reveal a higher plaeoproductivity and hence, a warm-humid climate. In the recent deposits, the selected geochemical proxies have not shown significant deviations which may be linked with a transitioning climate.

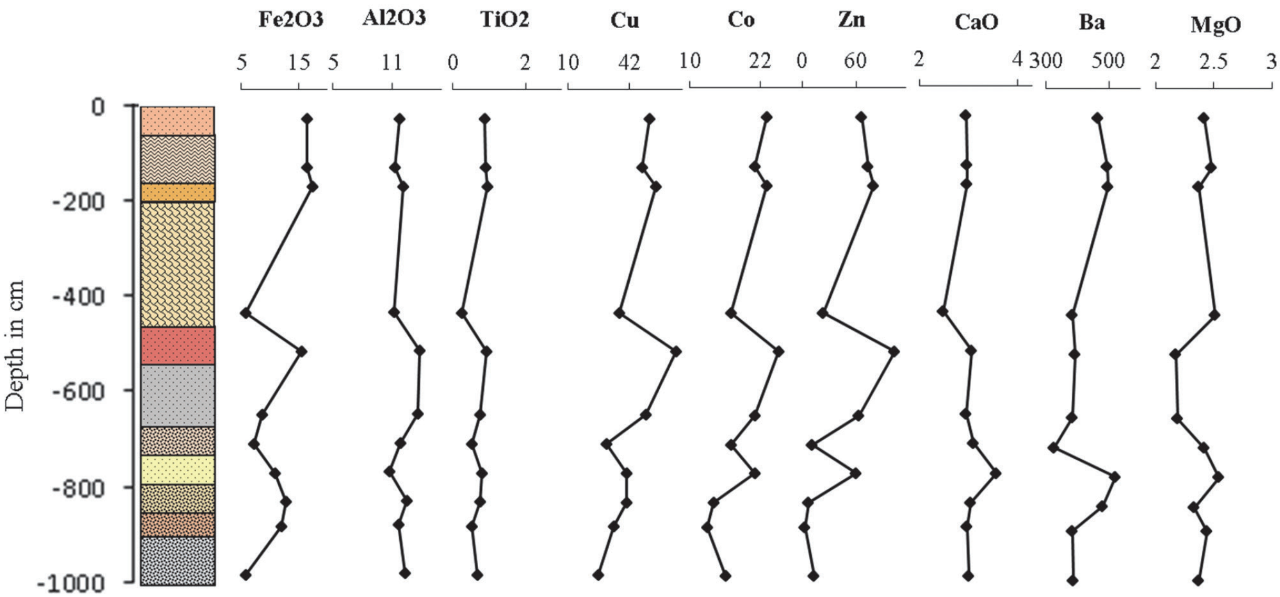

Figure 3: Down-core variation of terrestrial flux at JP site.

Variations in Weathering and Salinity

The geochemical proxies in the basal layers indicate a lower weathering, which can be associated with the cold-dry phase (Figure 5) as during cold-dry climate the rate of chemical weathering tend to decrease (Foster and Vance, 2007). An increase in the ratio of FeO/Al_2O_3, TiO/Al_2O_3, and MgO/Al_2O_3 in JPS8 can be the result of an enhanced weathering which can be due to a relatively warm and humid climate. Another episode of relatively lower weathering is marked in JPS6 which can be the result of a transitioning climate. The geochemical proxies have suggested a higher weathering during the deposition of JPS5, revealing a warm-humid climate. The ratios of FeO/Al_2O_3 and TiO_2/Al_2O_3 have illustrated decline in weathering during the deposition of JPS4, which can be attributed to a cold-dry episode. In JPS3, another phase of elevated weathering has occurred suggesting a warm-humid climate. In JPS2 and JPS1, no significant change in weathering has been marked.

The salinity index (MgO/CaO+MgO) has revealed low to moderate level of salinity at this location (Figure 5). The decline in salinity in JPS8 can be associated

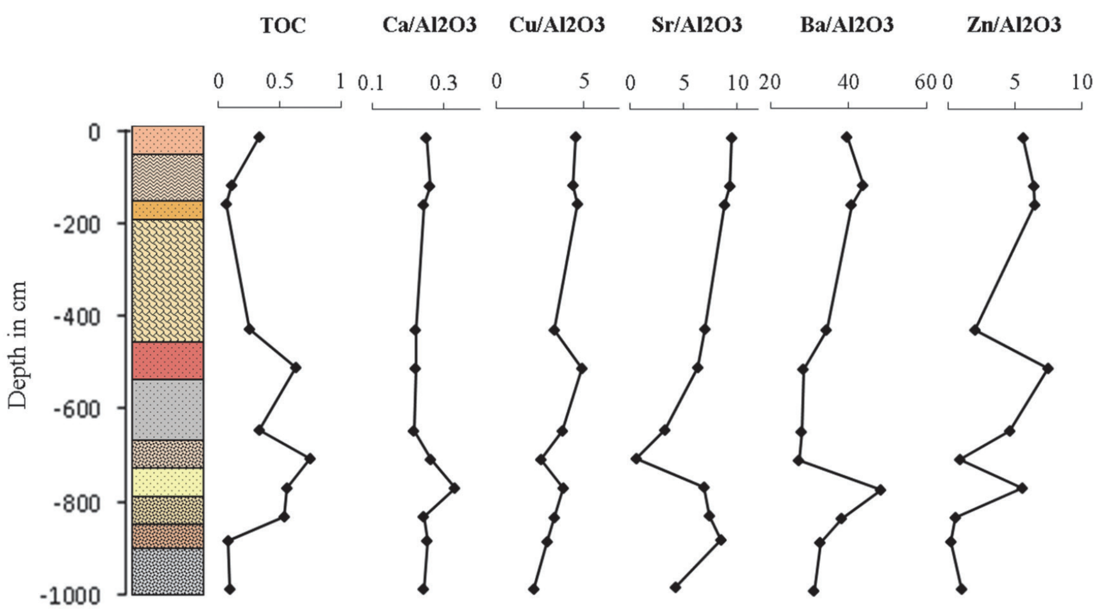

Figure 4: Down-core variation of paleoproductivity at JP site.

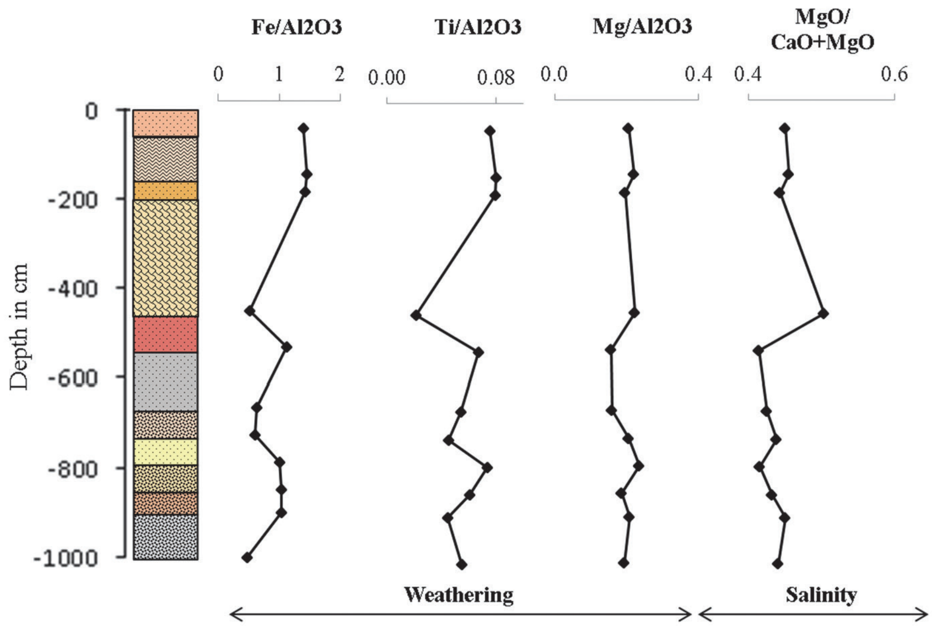

Figure 5: Variability in the proxies indicating weathering and salinity at JP site.

with a relatively higher humidity under a warm-humid climate. The salinity has declined considerably in JPS5 suggesting a higher humidity and hence, a warm-humid climate. The salinity variations also help in examining the changes in alkalinity (Cai et al., 2010; Saraswat et al., 2015). In JPS4, substantial increase in salinity illustrates episode of lower humidity under a cold-dry climatic episode. In JPS3, the salinity declined considerably demonstrating an enhanced humidity under a warm-humid climate. In JPS2 and JPS1, no remarkable change in salinity pattern has been observed.

From the above analysis, it is apparent that the region has gone through significant climatic changes in the past that was accompanied by sea level fluctuations owing to its proximity to the east coast of India (Banerjee, 2000; Khandelwal et al., 2008; Farooqui and Naidu, 2010; Jayagondaperumal et al., 2012; Limaye and Kumaran, 2012; Rao et al., 2015; Band et al., 2018).

The study has revealed that during the deposition of basal layers, the climate was comparatively cold and dry. The sediments deposited at this time are grayish and sandy suggesting an enhanced influence of marine processes in comparison to the fluvial. Khandelwal et al. (2008) in their study have also reported an elevated tidal action during 7900 cal yr BP in Chilikalake region. In other studies a sea transgression has been reported in the southeast coast around 7300 yr BP (Banerjee, 2000), 7900 cal yr BP (Khandelwal et al., 2008), and between 10,900 and 8800 cal yr BP (Rao et al., 2015). Hence, the JPS11 and JPS10 layers might have coincided with this phase of sea retreat. The climate became humid and warm during the deposition of JPS9 and JPS8. The sediments of JPS9 are orange with sandy clay texture, most probably indicating a transition phase. The yellow-clayey sequence of JPS8 has been associated with a warm-humid climate when the influence of tidal activity declined.

The accumulation of JPS8 might have occurred during the enhanced monsoon which has been reconstructed in the south-eastern coast around 6500 yr BP (Band et al., 2018). Another shift to a cold and dry climate occurred during the aggradation of JPS6. The sediments deposited during this episode are coarser that might be the result of a relatively higher tidal influence. The climate again became warm and humid as shown by the geochemical proxies during the sedimentation of JPS5. The clayey texture of this layer indicates deposition through fluvial action under a warm-humid climate. This phase of sedimentation most probably has occurred during sea retreat as reported during 2500 cal yr BP in the eastern coast (Banerjee, 1993; Banerjee, 2000; Khandelwal et al., 2008). Another episode of cold-dry climate occurred during the sedimentation of JPS4. Limaye and Kumaran (2012) have also reconstructed a weak monsoon and an arid climate between 3500 and 1500 BP in the south Konkan region. Similar observations have been made by Farooqui and Naidu, (2010), who have also reported a weak monsoon around 3000-2000 yr BP in the southeast coast.

The reddish gray-fine sand deposited in this layer has been attributed to the enhanced tidal action. Existence of a warm and humid climate has been exhibited by the geochemical proxies in JPS3 which might have been deposited during the enhanced monsoon episode since 2000 yr BP (Farooqui and Naidu, 2010).The finer texture of the sediments has indicated deposition through an elevated riverine action. The reddish-brown colour of JPS2 and JPS1 suggests predominance of fluvial/freshwater environment at the time of sediment accumulation. However, the geochemical proxies indicate a transitioning climate. Khandelwal et al. (2008) have reported a drier climate around 1600 cal yr BP in coastal Odisha. Similarly, Limaye and Kumaran (2012) have reconstructed a weak monsoon and an arid climate around 1500 BP in the south Konkan region.

Conclusion

The study was executed using a sediment core obtained from the flood plain of coastal Odisha, utilizing its colour, texture and geochemical proxies to deduce the paleoproductivity, terrestrial flux, weathering and salinity that indicate changes in the past climate. On the basis of selected geochemical proxies that the climate of the region has oscillated between distinct cold-dry and warm-humid phases. The proxies have shown the existence of a relatively cold-dry climate during the sedimentation of deeper layers, JPS11, JPS10 and JPS9. The climate became relatively warm and humid during the deposition of JPL8. A transition to cold-dry climate has been inferred during the aggradation of JPS6. The revival of a warm-humid climate occurred during the deposition of JPS5. During this phase, a notable decline in the tidal activity is also marked. A subsequent period of cold-dry climate with enhanced tidal influence has been marked during the deposition of JPS4. The proxies have suggested warm and humid conditions during the sedimentation of JPS3 while the analysis of JPS2 and JPS1 has indicated a climatic shift towards colder phase. Therefore, it can be concluded that using geochemical proxies, and physical attributes (colour and texture) of the sediment sequences, the paleoclimate of an area can be inferred.

Acknowledgements

The authors acknowledge the assistance of Advanced Instrumentation Research Facility (AIRF), Jawaharlal Nehru University in using the laboratory facilities for elemental analysis. The authors also acknowledge the soil laboratory of the Institute of Agriculture, Banaras Hindu University, Varanasi, Uttar Pradesh, India for their assistance in sediment organic carbon analysis.

References

Agnihotri, R., Sarin, M., Somayajulu, B., Jull, A. and Burr, G., 2003. Late-Quaternary biogenic productivity and organic carbon deposition in the eastern Arabian Sea. *Palaeogeography, Palaeoclimatology, Palaeoecology*, **197(1):** 43-60.

Alappat, L., Frechen, M., Ramesh, R., Tsukamoto, S. and Srinivasalu, S., 2011. Evolution of late Holocene coastal dunes in the Cauvery delta region of Tamil Nadu, India. *Journal of Asian Earth Sciences*, **42:** 381-397.

Alappat, L., Frechen, M., Sree Kumar, S., Suresh Babu, D.S., Ravur, R. and Tsukamot, S., 2015. Evidence of late Holocene shoreline progradation in the coast of Kerala, south India obtained from OSL dating of palaeo beach ridges. *Geomorphology*, **245:** 73-86.

Anderson, D.E., Goudie, A.S. and Parker, A.G., 2007. Global Environments through the Quaternary Exploring Environmental Change. Oxford University Press.

Babu, P.V.L.P., 1975. Morphological evolution of the Krishna delta. *Photonorvachak*, **3:** 21-27.

Banerjee, P.K., 1993. Imprints of late Quaternary climate and sea level changes on east coast and south Indian coast. *Geo-marine Letters*, **13:** 56-60.

Banerjee, P.K., 2000. Holocene and late Pleistocene relative sea level fluctuations along the east coast of India. *Marine Geology*, **167:** 243-260.

Banerji, U.S., Bhushan, R. and Jull, A.J.T., 2017. Mid-Late Holocene monsoonal records from the partially active mudflats of Diu island, southern Saurashtra Gujarat, western India. *Quaternary International*, **443(B):** 200-210.

Basavaiah, N., Mahesh Babu, J.L.V., Gawali, P.B., Naga Kumar, K.Ch.V., Demudu, G., Prizomwala, S.P., Hanamgond, P.T. and Rao, K.N., 2015. Late quaternary environmental and sea level changes from Kollerulake, SE India: Influences from mineral magnetic, geochemical and texture analysis. *Quaternary International*, **371:** 197-208.

Cai, W.J., Hu, X., Huang, W.J., Jiang, L.Q., Wang, Y., Peng, T.H. and Zhang, X., 2010. Alkalinity distribution in the western North Atlantic Ocean margins. *Journal of Geophysical Research*, **115:** 1-15.

Chauhan, O.S., Borole, D.V., Gujar, A.R., Mascarenhas, A., Mislankar, P.G. and Rao, Ch.M., 1993. Evidence of climatic variations during Late Pleistocene-Holocene in the eastern Bay of Bengal. *Current Science*, **65:** 558-562.

Coltorti, M., Melis, E. and Patta, D., 2010. Geomorphology, stratigraphy and facies analysis of some Late Pleistocene and Holocene key deposits along the coast of Sardinia (Italy). *Quaternary International*, **222:** 19-35.

Das, A., Prizomwala, S., Makwana, N. and Thakkar, M., 2017. Late Pleistocene-Holocene climate and sea level changes inferred based on the tidal terrace sequence, Kachchh, Western India. *Palaeogeography, Palaeoclimatology, Palaeogeography*, **473:** 82-93.

Farooqui, A. and Naidu, T.Y., 2010. The camoebians and palaeonological assemblage in Gautami-Godavari river mouth, India: Environment and sea level since 3000 years. *Journal of Geological Society of India*, **75:** 841-850.

Foster, G.L. and Vance, D., 2007. Negligible glacial-interglacial variations in continental chemical weathering rates. *Nature*, **444:** 918-921.

Goldberg, E.D. and Arrhenius, G., 1958. Chemistry of Pacific pelagic sediments. *Geochimica et Cosmochimica Acta*, **13(2):** 253-362.

Govil, P., Mazumder, A., Tiwari, A. and Kumar, S. 2016. Holocene climate variability from lake sediment core in Larsemann Hills, Antarctica. *Journal of the Geological Society of India*, **78(1):** 453-463.

Gredilla, A., Stoichev, T., de Vallejuelo, F.O. and Iruretagoiena, A.R., 2015. Spatial distribution of some trace and major elements in sediments of the Cavado estuary (Esposende, Portugal). *Marine Pollution Bulletin*, **99:** 305-311.

Haiyan, J., Jianfang, C., Huanxin, W., Hongliang, L., Weiyan, Z., Jie, X., Youcheng, B. and Kui, W., 2010. Variations in paleoproductivity and the environmental implications over the last six decades in the Changjiang Estuary. *Acta Oceanoogical Sinica*, **29(3):** 38-45.

Hameed, A., Achyuthan, H. and Sekhar, B., 2006. Radiocarbon dates and Holocene sea level change along the Cuddalore and Odinur coast, Tamil Nadu. *Research Communications*, **91(3):** 362-367.

Hodgson, D.A., McMinn, A., Kirkup, H., Cremer, H., Gore, D., Melles, M., Roberts, D. and Montiel, P., 2003. Colonization, succession, and extinction of marine floras during glacial cycle: A case study from the Windmill island (East Antarctica) using biomarkers. *Paleoceanography*, **18**. http://dx.doi.org/10.1029/2002PA000775.

Islam, M.S. and Tooley, M.J., 1999. Coastal and sea-level changes during the Holocene in Bangladesh. *Quaternary International*, **55(1):** 61-75.

Jayangondaperumal, R., Murari, M.K., Sivasubramanian, P. and Chandrasekar, N., 2012. Luminescence dating of fluvial and coastal red sediments in the SE coast, India, and implications for palaeoenvironmental changes and dune reddening. *Quaternary Research*, **77(3):** 468-481.

Jayalakshmi, K., Nair, K.M. and Santosh, M., 2004. Late Pleistocence-Holocene paleoclimatic history of the southern Kerala Basin, southwest India. *Gondwana Research*, **7(2):** 585-594.

Juyal, N., Kar, A., Rajaguru, S.N. and Singhvi, A.K., 2003. Luminescence chronology of Aeolian deposition during the Late Quaternary on the southern margin of Thar Desert, India. *Quaternary International*, **104:** 87-98.

Khandelwal, A., Mohanti, M., Rodrigues, F.G. and Schrf, B.W., 2008. Vegetation history and sea level variations during the last 13,500 years inferred from a pollen record at Chilika Lake, Orissa, India. *Vegetation History Archaeobotanist*, **17:** 335-344.

Kobayashi, D., Yamamoto, M., Irino, T., Nam, S., Park, Y., Harada, N., Nagashima, K., Chikita, K. and Saitoh, S., 2016. Distribution of detrital minerals and sediment color in western Arctic Ocean and northern Bering Sea sediments: Changes in the provenance of western Arctic Ocean sediments since the last glacial period. *Polar Science*, **10(4):** 519-531.

Koukina, S.E., Lobus, N.V., Peresypkin, V.I., Dara, O.M. and Smurov, A.V., 2017. Abundance, distribution and bioavailability of major and trace elements in surface sediments from the Cai River estuary and Nha Trang Bay (South China Sea, Vietnam). *Estuarine, Coastal and Shelf Science*, **198:** 450-460.

Krishna, J., 2017. The Indian Mesozoic Chronicle, Sequence Stratigraphic Approach. Springer, Singapore.

Kumaran, K.P.N., Nair, K.M., Shindikar, M., Limaye, R.B. and Padmalal, D., 2005. Stratigraphical and palynological appraisal of the late Quaternary mangrove deposits of the west coast of India. *Quaternary Research*, **64:** 418-431.

Li, T., Sun, G., Yang, C., Liang, K., Ma, S., Huang, L. and Luo, W., 2019. Source apportionment and source to sink transport of major and trace elements in coastal sediments: Combining positive matrix factorization and sediment trend analysis. *Science of the Total Environment*, **651:** 344-356.

Limaye, R.B. and Kumaran, K.P.N., 2012. Mangrove vegetation response to Holocene climate change along Konkan coast of south-western India. *Quaternary International*, **263:** 114-128.

Limaye, R.B., Padmalal, D. and Kumaran, K.P.N., 2014. Mangrove habitat dynamics in response to Holocene sea level and climate change along southwest coast of India. *Quaternary International*, **325:** 116-125.

Liu, D., Lin, B., Kandasamy, S., Wang, H., Liu, Q., Zou, W., Zou, J. and Shi, X., 2019. Geochemical appraisal of chemical weathering and metal contamination in coastal surface sediments, off northwest Hainan island, the Gulf of Tonkin. *Frontiers in Marine Sciences*, doi.org/10.3389/fmars.2019.00363.

Makwana, N., Prizomwala, S.P., Chauhan, G., Phartiyal, B. and Thakkar, M.G., 2019. Late Holocene paleo-environmental change in the Banni plains, Kachchh, Western India. *Quaternary International*, **507:** 197-205.

Malik, J.N., Banerjee, C., Khan, A., Johnson, F.C., Shishikura, M., Satake, K. and Singhvi, A.K., 2015. Stratigraphic evidence for earthquakes and tsunami on the west coast of South Andaman Island, India during past 1000 years. *Tectonophysics*, **661:** 49-65.

Mohtadi, M. and Hebbeln, D., 2004. Mechanisms and variations of the paleoproductivity off northern Chile (24 0S-33 0S) during the last 40,000 years. *Paleoceanography*, **19:** 2023. Doi: 10.1029/2004PA001003.

Munsell, A.H., 1947. A Colour Notation (10^{th}ed.). Munsell Color Company, Baltimore.

Naguib, M. and Bedaiwy, A., 2012. A simplified approach for determining the hydrometer's dynamic settling depth in particle size analysis. *Catena*, **97:** 95-103.

Nair, K.M., Padmalal, D., Kumaran, K.P.N., Sreeja, R., Limaye, R.B. and Srinivas, R., 2010. Late quaternary evolution of Ashtamudi-Sasthamkotta lake systems of Kerala, south west India. *Journal of Asian Earth Sciences*, **37:** 361-372.

Narayana, A.C., Prakash, V., Gautam, P.K. and Tripathi, S., 2017. Holocene environmental changes as recorded in sediments of a paleodelta, southwest coast of India. *Quaternary International*, **443(3):** 115-123.

Rao, K.N., Saito, Y., Nagakumar, K.C.V., Demudu, G., Basavaiah, N., Rajawat, A.S., Tokanai, F., Kato, K. and Nakashima, R., 2012. Holocene environmental changes of the Godavari delta, east coast of India, inferred from sediment core analysis and AMS ^{14}C dating. *Geomorphology*, **44:** 47-66.

Rao, K.N., Saito, Y., Nagakumar, K.Ch.V., Demudu, G., Rajawat, A.S., Sumiko Kubo, S. and Zhen Li, Z., 2015. Palaeogeography and evolution of the Godavari delta, east coast of India during the Holocene: An example of wave dominated and fan delta setting. *Palaeogegraphy, Palaeoclimatology*, *Palaeoecology*, **440:** 213-233.

Sageman, B.B. and Lyons, T.W., 2003. Geochemistry of fine grained sediments and sedimentary rocks. *In:* Sediments, Diagenesis and Sedimentary Rocks. Elsevier, 115-158. DOI: https://doi.org/10.1016/B0-08-043751-6/07157-7.

Saraswat, R., Kouthanker, M., Kurtarkar, S., Nigam, R., Naqvi, S.W.A. and Linshy, V.N., 2015. Effect of salinity induced pH/alkalinity changes on benthic foraminifera: A laboratory culture experiment. *Estuarine, Coastal and Shelf Science*, **153:** 96-107.

Sayem, A.S.M., Guo, Z., Wu, H., Zhang, C., Yang, F., Xiao, G. and He, Z., 2018. Sedimentary and geochemical evidence of Eocene climate change in the Xining Basin, northeastern Tibetan Plateau. *Science China Earth Sciences*, **61(9):** 1292-1305.

Schneider, R.R., Price, B., Muller, P.J., Kroon, D. and Alexander, I., 1997. Monsoon related variations in Zaire (Congo) sediment load and influence of fluvial silicate supply on marine productivity in the east equatorial Atlantic during the last 200,000 year. *Paleooceanography*, **12(3):** 463-481.

Selvakumar, V., Rajaguru, S.N. and Jhaldiyal, R., 2012. Palaeolithic occupation of southern Tamil Nadu, India: New evidence from south of the river Kaveri. *Quaternary International*, **269:** 74-86.

Singh, S., Prakash, B., Awasthi, A.K. and Kumar, S., 2014. Do stable isotopes in carbonate cement of Nio-Pleistocene Himalayan sediments record paleogeological and paleoclimatic changes? *Palaeogeography, Palaeoclimatology, Palaeoecology*, **399:** 363-372.

Srivastava, J. and Farooqui, A., 2013. Late Holocene mangrove dynamics and coastal environmental changes in the Northeastern Cauvery River Delta, India. *Quaternary International*, **298:** 45-56.

Tribovillard, N., Algeo, T.J., Lyons, T. and Riboulleau, A., 2006. Trace metal as paleoredox and paleoproductivity proxies: An update. *Chemical Geology*, **232(1):** 12-32.

Tripathi, G.R., Singh, S.K. and Ramaswamy, V., 2014. Major and trace element geochemistry of Bay of Bengal sediments: Implications to provenances and their controlling factors. *Palaeogeography, Palaeoclimatology, Palaeoecology*, 397: 20-30.

Vaz, G.G. and Banerjee, P.K., 1997. Middle and Late Holocene sea level changes in and around Pulicat lagoon, Bay of Bengal, India. *Marine Geology*, **138:** 261-271.

Walkley, A. and Black, I.A., 1934. Chemical soil tests. Cornell University. *Agricultural Expedition Experiment Station Buletine*, **960:** 34-36.